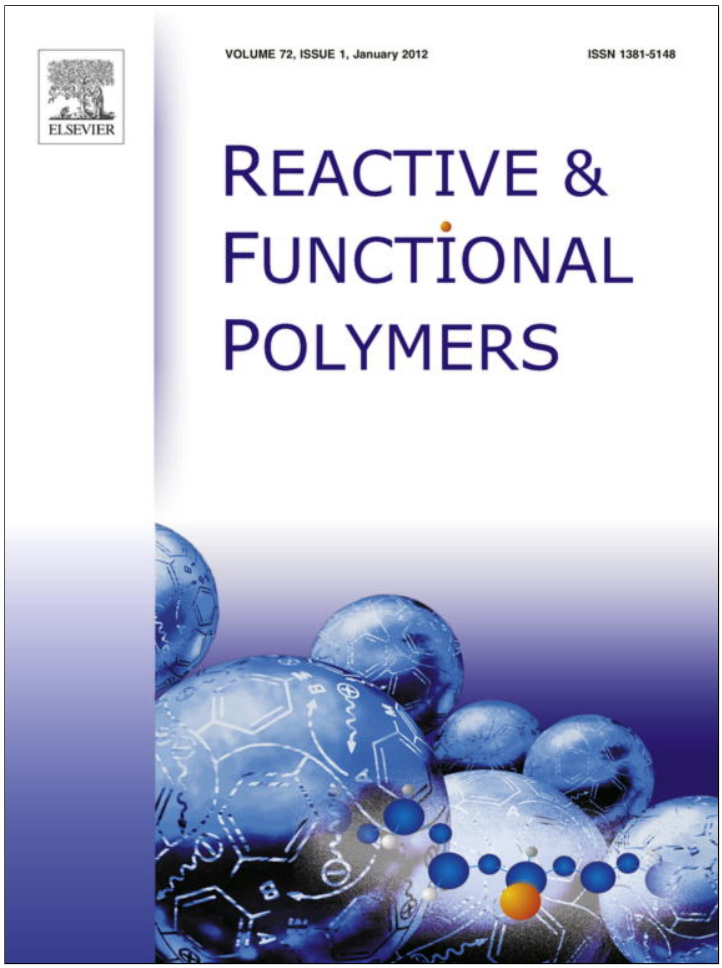

(This is a sample cover image for this issue. The actual cover is not yet available at this time.)

Reactive & Functional Polymers 73 (2013) 442–450

Contents lists available at SciVerse ScienceDirect

Reactive & Functional Polymers

journal homepage: www.elsevier.com/locate/react

Ethidium bromide binding to DNA cryogels

Pinar Karacan, Oguz Okay *

Istanbul Technical University, Department of Chemistry, 34469 Istanbul, Turkey

ARTICLE INFO

Article history:
Received 25 July 2012
Received in revised form 23 November 2012
Accepted 25 November 2012
Available online 3 December 2012

Keywords:
DNA
Cryogels
Ethidium bromide
Binding
Swelling

ABSTRACT

The interaction of the classical intercalator ethidium bromide (EtBr) with the double helical network strands of DNA cryogels was investigated. The cryogels were prepared starting from aqueous solutions of DNA (about 2000 base pairs long) at −18 °C using 1,4-butanediol diglycidyl ether crosslinker under various reaction conditions. In contrast to the solubilization of DNA hydrogels in aqueous EtBr solutions, DNA cryogels remain stable even after complete saturation of their EtBr binding sites. The total binding capacity of the cryogels is 0.6 ± 0.1 EtBr per nucleotide, which is close to the theoretical maximum number of EtBr molecules that can bind to DNA. Even in very dilute solutions (down to 3 μM), cryogels remove EtBr from aqueous solutions with an efficiency of 90%. The equilibrium binding constant and the maximum number of EtBr binding sites of the cryogels almost coincide with the reported values for the secondary binding process of EtBr by DNA in aqueous solutions. At low mole ratios of bound EtBr to DNA, the cryogels swell with increasing amount of bound EtBr, most likely caused by the lengthening of DNA due to the intercalated EtBr. The response of DNA cryogels to changes in EtBr concentration between 3 and 300 μM also suggests that they can be used to detect DNA binding substrates in aqueous solutions.

1. Introduction

Deoxyribonucleic acid (DNA) serves as the carrier of genetic information in living organisms and is composed of building blocks called nucleotides consisting of deoxyribose sugar, a phosphate group and four bases, adenine, thymine, guanine, and cytosine. DNA has a double-helical (ds) conformation in its native state which is stabilized by hydrogen bonds between the bases attached to the two strands [1]. When a DNA solution is subjected to high temperatures, the hydrogen bonds holding the two strands together break and the double helix dissociates into two single strands (ss) having a random coil conformation [2].

DNA hydrogel is a network of chemically crosslinked DNA strands swollen in aqueous solutions [3,4]. Such soft materials are a good candidate to make use of the characteristics of DNA such as coil-globule transition, biocompatibility, selective binding, and molecular recognition [5,6]. DNA hydrogels were prepared starting from branched DNA molecules via ligase-mediated reactions [7]. These hydrogels can also be prepared by crosslinking of DNA in aqueous solutions at 50 °C using diepoxides as chemical crosslinking agents [8]. Epoxide groups can react with the amino groups on the nucleotide bases to form heat resistant interstrand crosslinks leading to the formation of a three dimensional DNA network. DNA hydrogels are responsive systems exhibiting drastic volume changes in response to the external stimuli, such as acetone [8,9], polyethylene glycol [10], inorganic salts [11–14], polyamines [12,13], cationic macromolecules [15], or surfactants [12,13,16]. Responsive DNA hydrogels with a wide range of tunable properties such as the conformation of the network strands [10], viscoelasticity [17], nonlinear elasticity (strain hardening) [18], and porosity have been prepared in the past few years [19]. Recently, by conducting the gelation reactions at subzero temperatures, macroporous DNA cryogels with excellent mechanical properties have been obtained [19]. It was shown that such soft materials consisting of only DNA strands can be used for the removal of carcinogenic agents from aqueous solutions.

The interaction of various ligands with DNA occurs in several ways such as covalent, non-covalent, intercalative, or electrostatic binding [20–22]. Intercalation involves the insertion of a planar molecule between DNA base pairs, which results in a decrease in the DNA helical twist and lengthening of the DNA [23,24]. DNA intercalators are useful as biochemical tools for the visualization of DNA, and have been used extensively as antitumor drugs. The classical intercalator ethidium bromide (EtBr) is a four-ringed aromatic molecule with three of the rings conjugated. The nature of the interaction of EtBr with DNA has been examined by a variety of techniques over the past 50 years [25–33]. It is generally recognized that the strong mode of binding of EtBr to ds-DNA results in the intercalation of the planar phenanthridium ring between adjacent base pairs on the double helix. The intercalation of EtBr both increases the distance between base pairs by 0.3 nm and unwinds

* Corresponding author. Tel.: +90 212 2853156; fax: +90 212 2856386.
E-mail address: okayo@itu.edu.tr (O. Okay).

1381-5148/$ - see front matter © 2012 Elsevier Ltd. All rights reserved.
http://dx.doi.org/10.1016/j.reactfunctpolym.2012.11.014

the double helix by 26° causing increasing length of the DNA [34,35]. Moreover, at high concentrations, EtBr also interacts with DNA by electrostatic interactions.

The aim of this study is to explore how the properties of DNA gels vary with the binding ratio of EtBr to DNA nucleotide. It was also of inherent interest to determine the number of EtBr binding sites per nucleotide and the binding capacity of DNA gels. Although numerous works has been published in the literature on EtBr–DNA interactions in aqueous solutions, the present study is the first to investigate these interactions inside a gel phase. Our preliminary experiments showed that DNA hydrogels, that are stable in water, gradually dissolve in EtBr solutions, probably due to the increasing length of DNA strands. In contrast, DNA cryogels immersed into these solutions remained stable even after complete saturation of their EtBr binding sites. Therefore, in the present study, cryogels were used to investigate EtBr–DNA interactions and the resulting changes in the swelling behavior of the gels. The paper is organized as follows: We first describe the optimum design of ds-DNA cryogels by changing the synthesis parameters. In our previous work [19], DNA cryogels were prepared in the form of beads in paraffin oil as the continuous phase. To eliminate the effect of the impurities coming from the oil phase and, due to bead-to bead variation of the gel properties, DNA cryogels were prepared in this study in closed reactors. This new procedure also provided detailed characterization of the cryogels. 1,4-Butanediol diglycidyl ether (BDDE) was used as a crosslinker and TEMED as a catalyst in the gel preparation. Cryogels consisting of ds-DNA strands were then subjected to EtBr binding studies in aqueous EtBr solutions. Equilibrium data were also obtained at various mole ratios of bound EtBr to nucleotide and the results were compared with those obtained in aqueous DNA solutions.

2. Experimental

2.1. Materials

Cryogels were made from deoxyribonucleic acid sodium salt from salmon testes (DNA, Sigma). According to the manufacturer, the % G–C content of the DNA used is 41.2%, and the melting temperature is reported to be 87.5 °C in 0.15 M sodium chloride plus 0.015 M sodium citrate. The molecular weight determined by ultracentrifugation is 1.3×10^6 g/mol, which corresponds to approximately 2000 base pairs. The crosslinker 1,4-butanediol diglycidyl ether (BDDE, Aldrich), N,N,N′,N′-tetramethylethylenediamine (TEMED, Merck), ethidium bromide (Fluka), acridine orange (Aldrich), and sodium bromide (NaBr, Merck) were used as received. Stock solution of TEMED was prepared by dissolving 0.528 ml TEMED in 20 ml 4.0 mM NaBr.

2.2. Preparation of DNA cryogels

The cryogelation reactions were carried out at −18 °C for 2 or 3 days. The concentrations of DNA, BDDE, and TEMED were varied over a wide range to determine the optimum condition for cryogel formation. In the following, these concentrations with respect to the reaction volume were denoted by C_{DNA} (w/v%), C_{BDDE} (w/v%), and C_{TEMED} (v/v%), respectively. DNA was first dissolved in 4.0 mM NaBr at 35 °C for 1 day. After addition of BDDE and stirring for 1 h, TEMED was included into the reaction solution. The solution was then transferred into several plastic syringes of 4.5 mm internal diameters. To prevent denaturation of DNA due to the effect of TEMED [10,19], the syringes were immediately immersed in liquid nitrogen for 1–2 min, and then, they were placed in a cryostat at −18 °C for 2 or 3 days to complete the cryogelation reactions. For comparison, hydrogels of DNA were also prepared, as described before [10,19], from 9.3% DNA solutions in the presence of 0.44% TEMED and 1.0% BDDE at 50 °C for 4 h.

2.3. Swelling measurements

DNA cryogels taken from the syringes were cut into samples of about 5 mm in length. Then, each sample was placed in an excess of 4.0 mM aqueous NaBr solution. In order to reach swelling equilibrium, the sample was immersed in solution for one week replacing the solution many times. The swelling equilibrium was tested by monitoring the diameter of the gels using an image analyzing system consisting of a microscope (XSZ single Zoom microscope), a CDD digital camera (TK 1381 EG) and a PC with the data analyzing system Image-Pro Plus. The swelling equilibrium was also tested by weighing the gel samples. Thereafter, the equilibrium swollen gels were frozen at −86 °C for 1 day before being freeze-dried at −40 °C/0.12 mbar for 1 day and −60 °C/0.01 mbar for an additional 1 day. The equilibrium volume and the equilibrium weight swelling ratios, q_v and q_w, respectively, were calculated as:

$$q_v = (D/D_{dry})^3 \tag{1}$$

$$q_w = m/m_{dry} \tag{2}$$

where D and D_{dry} are the diameters of the equilibrium swollen and dry gels, respectively, m and m_{dry} are the weights of gels after equilibrium swelling and after drying, respectively. The swelling measurements were conducted on at least 6 gel samples prepared under the same experimental condition and the results were averaged. The gel fraction W_g, that is, the mass of crosslinked DNA obtained from 1 g of DNA was calculated from the masses of dry, extracted DNA network and from the DNA mass in the feed.

For the deswelling kinetics measurements, the equilibrium swollen gels in 4.0 mM NaBr solution were immersed in acetone at 24 °C. Gel volume changes were measured in situ by following the diameter of the samples under microscope using the image analyzing system. For the measurement of the swelling rates, the collapsed gels in acetone were transferred into 4.0 mM NaBr at 24 °C. The diameter changes were also monitored as described above. The results were given as the relative volume swelling ratio:

$$V_{rel} = (D_t/D)^3 \tag{3}$$

where D_t is the gel diameter at time t.

2.4. Mechanical tests

Uniaxial compression measurements were performed at 24 °C on cryogel samples in their swollen states. The stress–strain isotherms were measured by using an apparatus previously described [36]. Briefly, a cylindrical gel sample of about 6 mm in diameter and 5 mm in length was placed on a digital balance (Sartorius BP221S, readability and reproducibility: 0.1 mg). A load was transmitted vertically to the gel through a rod fitted with a PTFE endplate. The compressional force acting on the gel was calculated from the reading of the balance. The resulting deformation was measured by using a digital comparator (IDC type Digimatic Indicator 543-262, Mitutoyo Co.), which was sensitive to displacements of 10^{-3} mm. The elastic modulus G was determined from the initial slope of linear dependence:

$$\sigma_{nom} = G(\lambda - \lambda^{-2}) \tag{4}$$

where σ_{nom} is the nominal stress, i.e., the force acting per unit cross-sectional area of the undeformed gel specimen, and λ is the deformation ratio (deformed length/initial length).

2.5. Texture determination and porosity of cryogels

For the texture determination of freeze-dried cryogels, scanning electron microscopy (SEM) studies were carried out at various magnifications between 50 and 2000 times (Jeol JSM 6510LV Field Emission SEM). Prior to the measurements, network samples were sputter-coated with gold for 3 min using Sputter-coater S150 B Edwards instrument. The pore volume V_p of the cryogels was estimated through uptake of methanol of the swollen gel samples. The gels swollen in 4.0 mM NaBr were transferred into methanol and methanol was refreshed several times until the gel mass remains unchanged. Since methanol is a nonsolvent, it only enters into the pores of the DNA network. Thus, V_p (ml pores in one gram of dry DNA network) was estimated as:

$$V_p = (m_M - m_{dry})/(d_M m_{dry}) \quad (5)$$

where m_M is the gel mass immersed in methanol and d_M is the density of methanol (0.792 g/ml).

2.6. ATR-FTIR measurements

Spectra of the freeze-dried cryogel samples were collected using a single bounce diamond attenuated total refractance (ATR) module on a Fourier-transform infrared (FTIR) spectrometer (Nicolet Nexus 6700) equipped with a liquid nitrogen cooled mercury–cadmium–telluride (MCT) detector. The resolution of each spectrum was 4 cm^{-1}, and 64 interferograms were coadded in the range of 500–4000 cm^{-1}.

2.7. Acridine orange staining of gels

Swollen gel samples were immersed in acridine orange solutions (68 μg/ml) for 1–2 min, then washed with water, and stained gel samples were examined under UV light at 366 nm.

2.8. EtBr binding studies

Solutions of EtBr (3 μM–1 mM) were prepared by dissolving EtBr in distilled water and diluting stock solutions. EtBr binding to the gel samples was monitored by the decrease of absorbance of the solutions at 479 nm on a T80 UV-visible spectrometer. For the concentration range below 0.18 mM EtBr, the molar extinction coefficient (ε_{479}) at 479 nm was found to be 5500 M^{-1} cm^{-1}, which is in accord with the reported values [30]. Kinetic EtBr binding tests were conducted using swollen gel pieces containing about 0.15 mmol nucleotides. Each gel sample was immersed in 190 ml of 0.2 mM EtBr, corresponding to EtBr-to-DNA mole ratio of 0.25, and EtBr binding was monitored for a duration of 3 days. To obtain the equilibrium data, gel pieces (12–18 μmol nucleotides) were immersed into several EtBr solutions of 20 ml in volume but different concentrations between 2.5 μM and 0.5 mM, corresponding to EtBr-to-DNA mole ratios from 0.005 to 1.3. It was found that 5 days of contact time between EtBr and cryogels suffice to reach the equilibrium between the gel and solution phases. Then, EtBr concentration in equilibrium with gels was determined. From the initial and equilibrium concentrations of EtBr together with the moles of nucleotide used in the experiments, bound EtBr per nucleotide, denoted by r, was calculated. The equilibrium binding constant and the maximum number of sites per nucleotide were estimated from the Scatchard plot [37].

3. Results and discussion

We discuss the results of our experiments in two subsections. The first subsection deals with the optimization of the cryogelation conditions of DNA to obtain high-toughness gels consisting of ds-DNA network chains. In the second subsection, the interaction of EtBr with DNA cryogels is discussed and experimental observations are interpreted by comparing with the reported values for aqueous DNA solutions.

3.1. Cryogel properties

DNA cryogels were prepared starting from aqueous DNA solutions containing BDDE crosslinker and TEMED catalyst. NaBr (4 mM) was included into the gelation solutions to stabilize the DNA helical structure with respect to the dissociation into single strands [38]. After freezing of the gelation solutions and keeping at −18 °C for 3 days, cryogels with various properties were obtained depending on the synthesis parameters. The reaction mechanism of gel formation seems to involve the amino groups on the nucleotide bases, which attack sterically more accessible β-carbon of the epoxide of BDDE [39]. The reaction between epoxides and DNA is of nucleophilic substitution type (S_N2 reaction) and occurs at the nucleophilic sites in DNA, mainly at the N7 position of guanine [15,17,39,40]. It is thought that, under cryogelation conditions, the reactions occur in the unfrozen domains of the semi-frozen DNA solution leading to the formation of interstrand BDDE crosslinks and, hence, DNA gelation. We fixed the cryogelation temperature at −18 °C, which was reported as the optimum temperature for obtaining many synthetic and biological cryogels [41–48]. The remaining synthesis parameters, namely the concentrations of DNA, BDDE, and TEMED were varied for the optimization of the cryogel properties.

Water-insoluble cryogels could not be obtained in the absence of TEMED while, with rising amount of TEMED, the gel fraction W_g rapidly increased and leveled off at around 0.22% TEMED corresponding to pH $\geqslant$ 10.3 (Fig. S1). This type of TEMED or pH dependence is reasonable given that the nucleophile reactions are promoted under basic solutions. In the following, TEMED content of the reaction solutions was fixed at 0.33%. The effects of the concentrations of DNA (C_{DNA}) and BDDE (C_{BDDE}) on the cryogel properties are illustrated in Fig. 1A, where the gel fraction W_g and the elastic modulus G of swollen cryogels are plotted as functions of C_{DNA} and C_{BDDE}. It is seen that a macroscopic DNA network starts to form after passing a critical amount of DNA or BDDE. An almost complete conversion of soluble to crosslinked DNA (W_g = 0.92 to 0.96) requires 3% DNA and 0.39% BDDE, corresponding to the presence of equimolar ratio of epoxy to DNA base pair in the gelation solutions. This high crosslinker level required for complete gelation suggests that the crosslinking reactions between the amino groups on the nucleotide bases and epoxide groups of BDDE are very slow. Indeed, experiments conducted to shorten the cryogelation time from 3 to 2 days resulted in lower gel fractions and lower elastic moduli of the cryogels (Fig. S2). Since DNA gelation using diepoxide crosslinkers occurs within hours at 50 °C [10], as compared to 3 days of gelation time in this study, the low cryogelation temperature seems to be responsible for slowing down of the crosslinking reactions. Fig. 1A also shows that, between C_{DNA} = 4% and 7%, the elastic modulus of the cryogels rapidly increases indicating formation of increasing number of elastically effective links between DNA strands.

The cryogels formed at various C_{DNA} and C_{BDDE} exhibited weight swelling ratios (q_w) between 40 and 130 indicating that they are in a highly swollen state with 98–99% water in the cryogel structure. However, volumetric measurements showed that the volume swelling ratios q_v of the cryogels are about one order of magnitude smaller than their weight swelling ratios q_w. This is illustrated in Fig. 1B by the filled symbols, where q_w and q_v are plotted, in a semi-logarithmic scale, against C_{DNA} and C_{BDDE}. Since the weight swelling includes water locating in both pores and in the polymer

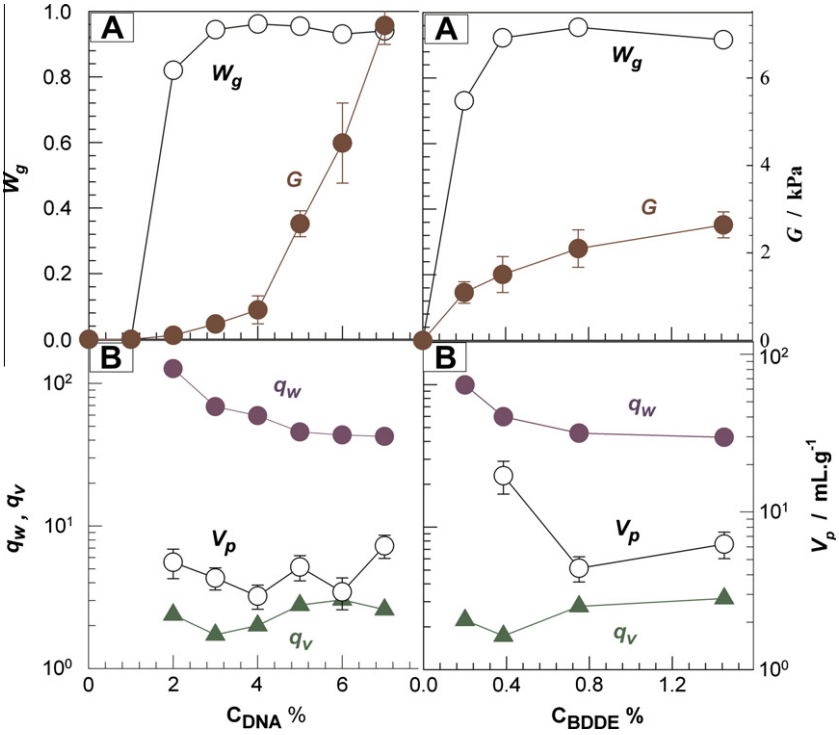

Fig. 1. Gel fraction W_g, elastic modulus G, equilibrium weight and volume swelling ratios, q_w and q_v, respectively, and the pore volume V_p of DNA cryogels shown as a function of C_{DNA} and C_{BDDE}. Gelation temperature = −18 °C. C_{TEMED} = 0.33%. Time = 3 days. A: BDDE = 15 wt% with respect to DNA. B: C_{DNA} = 5%.

region of the gel, while, assuming isotropic swelling, the volume swelling only includes water in the polymer region, the difference between q_w and q_v indicates the dry state porosity (macroporosity) of the cryogel networks [49]. The total porosity P (volume of open pores/volume of DNA network) of the cryogels was estimated from their q_w and q_v values using the equation $P = 1 - q_v/q_w$ [49]. The results show that P equals to 93–99% for all the cryogel samples. Open symbols in Fig. 1B represent the total volume of the pores V_p in the cryogels estimated from the uptake of methanol. The values V_p are between 3 and 20 ml/g indicating that the total pore volume of the cryogel samples is much larger than the bulk gel volume. This suggests that the main part of water in swollen cryogels is within the pores while the gel part making the pore walls is less swollen.

To visualize the pores in DNA cryogels, the network samples were investigated by scanning electron microscopy (SEM) with the assumption that the pore structure does not alter during freeze-drying due to the dense pore walls of the cryogels. Fig. 2 shows SEM images of the network samples prepared at 5% DNA and at various crosslinker contents. All the gel samples have a porous structure in dry state with irregular large pores of 10^1–10^2 μm in diameter. The macroporous structure of the cryogels is due to the presence of ice crystals acting as template (or, pore forming agent) during the gelation reactions [45,46,50]. We recently demonstrated that frozen hydrogel samples at temperatures between −10 °C and −24 °C contain 6% non-freezable water, which is bound to the polymer chains and remains unfrozen even at −24 °C [47]. The crosslinking reactions under cryogelation conditions only proceed in these unfrozen zones and lead to the formation of a polymer network with macroporous channels due to the presence of ice crystals. Interconnected open pore structure of DNA cryogels can also be demonstrated by the mechanical tests. Cryogels formed at 5% DNA can be compressed up to about 80% strain during which water inside the gels is removed. The compressed gels immediately swell in contact with water to recover its original shape. The process of filling and emptying the pores under force was perfectly reversible.

In Fig. 3A, large strain properties of the cryogel samples are illustrated as the dependence of the nominal stress on percent compression. Cryogels formed at a low concentration of DNA or BDDE exhibit relatively low compressive stresses, while those formed at 5% DNA are very tough and can be compressed up to about 80% strain without any crack development. These cryogels formed at $C_{BDDE} \geqslant 0.75\%$ also exhibit the largest compressive stresses (about 50 kPa). Fig. 3B represents the response rate of DNA cryogels formed at 5% DNA and at various crosslinker contents. Here, the normalized gel volume V_{rel} (volume of gel at time t/equilibrium swollen volume in 4.0 mM NaBr) is plotted against the time t of deswelling in acetone and re-swelling in aqueous 4 mM NaBr. Except for the gel formed at the highest crosslinker level, all the gel samples attain their equilibrium collapsed and equilibrium swollen states within 15 and 5 min, respectively. Moreover, they all exhibit completely reversible swelling–deswelling cycles, i.e., the gels return to their original shape and original mass after a short re-swelling period.

The above results thus reveal that the cryogels formed at 5% DNA and 0.75% BDDE exhibit high-toughness combined with a high mechanical strength, which will be used in the following section for the binding tests of EtBr from aqueous solutions. Before the tests, the conformation of the network chains was assessed by the ATR-FTIR spectra of freeze-dried cryogel samples. In Fig. 4A, the spectra of DNA networks formed at various C_{BDDE} are shown together with the spectra of ds-DNA before crosslinking and the crosslinker BDDE. The peak at 1220 cm^{-1} assigned to PO^{2-} antisymmetric stretching vibration is known to be invariant of DNA conformation and therefore, it was used for the normalization of the spectra [51]. The peaks at 1087 cm^{-1} and 1055 cm^{-1} corresponding to PO^{2-} symmetric stretching vibration and C–O stretching vibration of phosphodiester, respectively, characterize backbone conformation. The intensity of these peaks decreases

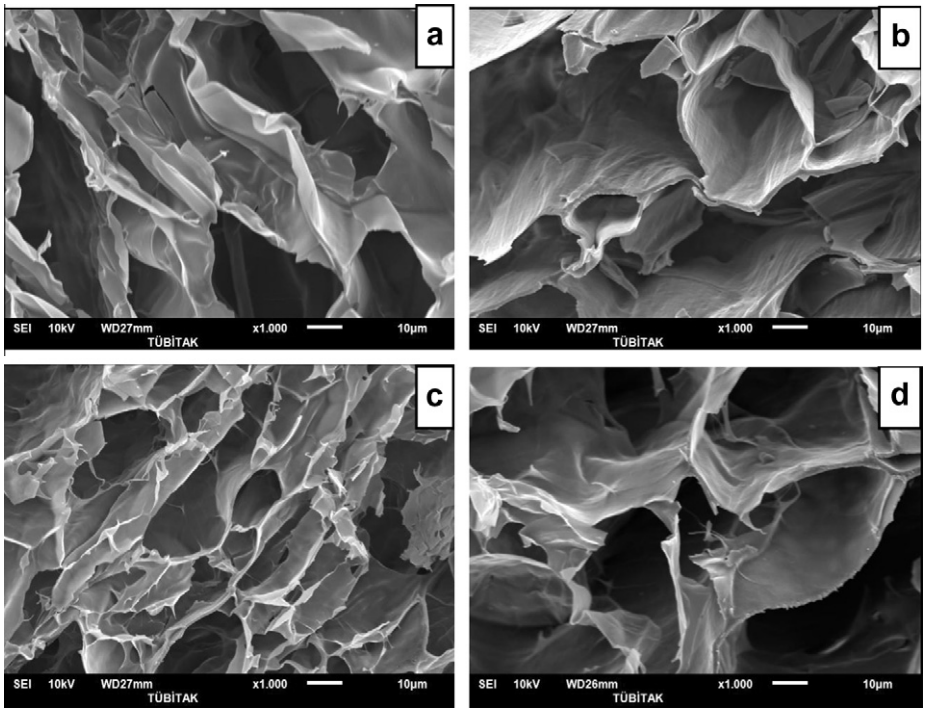

Fig. 2. SEM of dried DNA cryogels. C_{DNA} = 5%, C_{TEMED} = 0.33%, C_{BDDE} = 0.20% (a), 0.39% (b), 0.75% (c) and 1.45% (d). The scaling bars are 10 μm. Magnification = 1000×.

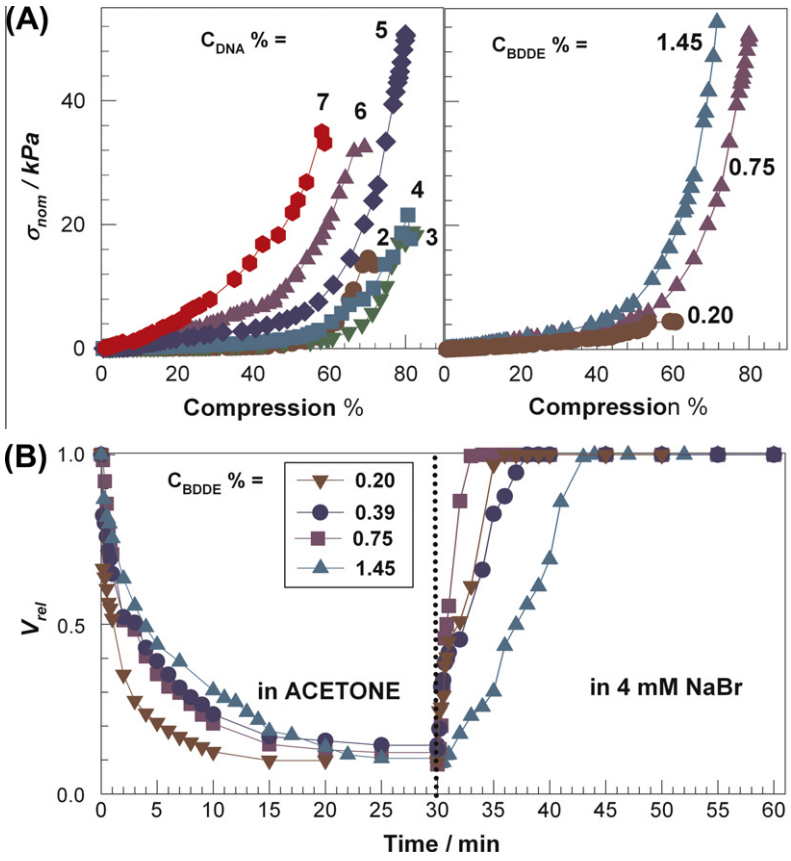

Fig. 3. (A) Stress–strain curves of the cryogels formed under various concentrations of DNA and BDDE indicated. See Fig. 1 caption for explanations. (B) Swelling–deswelling cycles of DNA cryogels shown as the variation of the relative gel volume V_{rel} with the time of deswelling in acetone and re-swelling in aqueous 4 mM NaBr. C_{DNA} = 5% and C_{BDDE}% indicated.

during denaturation due to the conformational changes in deoxyribose-phosphate backbone upon disruption of the DNA helical structure [51–53]. In contrast, we always observed an increased intensity of these peaks after the crosslinking reactions. This is

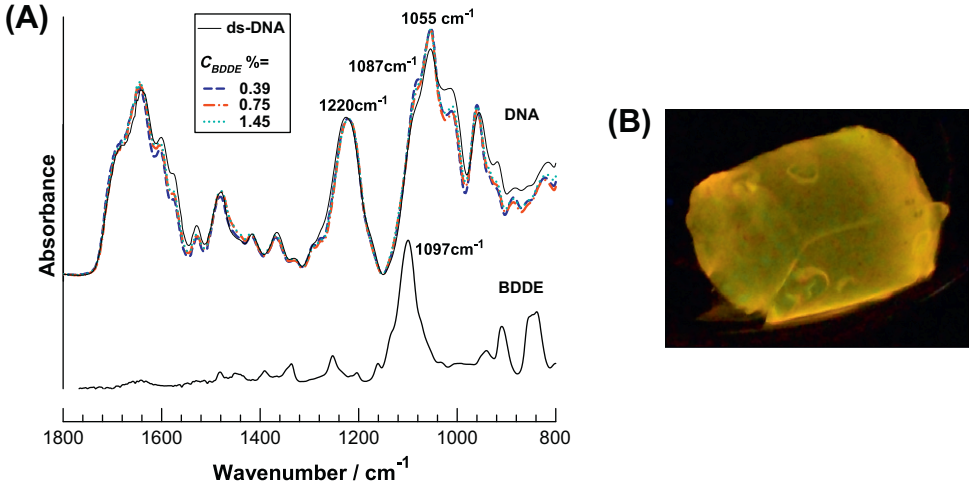

Fig. 4. (A) ATR-FTIR spectra of dried DNA cryogels formed at various C_{BDDE} indicated. C_{DNA} = 5%. For comparison, spectra of DNA before crosslinking, denoted by ds-DNA in the figure, and BDDE are also shown. (B) Image of a DNA cryogel sample, stained with acridine orange, under UV light at 366 nm. C_{DNA} = 5% and C_{BDDE} = 0.75%. (For interpretation of the references to color in this figure legend, the reader is referred to the web version of this article.)

attributed to C–O–C stretching of BDDE crosslinks, which appears in BDDE molecules at 1097 cm^{-1}, as also seen in Fig. 4A. The peaks in the range of 1550–1750 cm^{-1} characterizing base pairing and base stacking remain unchanged after crosslinking indicating that DNA conformation remains unchanged during the cryogelation reactions. The conformation of DNA was also checked by staining the cryogel samples with acridine orange and the stained samples were examined under UV light. As seen in Fig. 4B, the cryogels fluoresce green due to the monomeric acridine orange bound to double helical DNA network chains. In contrast, cryogels prepared from single stranded DNA strands, as described before [19], fluoresce red indicating predominantly ss-DNA conformation of their network chains.

3.2. Ethidium affinity of DNA cryogels

EtBr binding to DNA was investigated using cryogels formed at 5% DNA and 0.75% BDDE. Two series of experiments were carried out. First, the initial EtBr concentration in the external solution was fixed at 0.2 mM, corresponding to 0.25 EtBr molecule per nucleotide and, EtBr binding was monitored as a function of time for a duration of 3 days. Second, the contact time was set to 5 days to obtain the equilibrium data, while EtBr concentration in the solution was varied between 0.005 and 1.3 EtBr per nucleotide. To highlight the effect of the cryogel properties on the EtBr affinity, EtBr binding studies were also conducted using nonporous DNA hydrogels with ds-DNA conformation.

Fig. 5A shows EtBr concentration in the external solution ($C_{f,t}$) plotted against the contact time t with the cryogel and hydrogel of DNA. During the first 24 h, $C_{f,t}$ decreases with almost the same rate, and both gel samples bind 0.10–0.15 mol EtBr per mol of nucleotide. At longer times, hydrogel sample starts to disintegrate, as can be seen in the figure from the increase of EtBr concentration. After about 3 days, DNA hydrogel completely dissolved in EtBr solution. In contrast, DNA cryogel remains stable over the whole time period while absorbing continuously EtBr, during which the color of the solution changed from red[1] to clear (Fig. 5B). This highlights the stability of DNA strands in the cryogels and thus, demonstrates that DNA cryogels are effective sorbents as compared to DNA hydrogels. The cryogel samples subjected to nine successive sorption cycles in 0.2 mM EtBr solutions also remained stable in aqueous solutions. As seen in Fig. 5C, the color of the cryogel changes from clear to red during the first cycle and becomes dark red after seven cycles revealing increasing amount of bound EtBr in the cryogel.

The results of seven successive sorption cycles are shown in Fig. 6A, where $C_{f,t}$ is plotted against the contact time with the DNA cryogel. During the first two cycles, EtBr concentration decreases from 0.2 mM up to about 0.02 mM, i.e., 90% of EtBr in the solution is absorbed by the cryogel. The sorption capacity decreases in the following cycles and the cryogel saturates after six cycles. In Fig. 6B, the number of EtBr molecules bound per nucleotide, denoted by r, is plotted against the cumulative contact time of successive cycles. A rapid sorption of EtBr by the cryogel up to r = 0.45 followed by a slow sorption process is seen from the figure. Repeated tests showed that the total capacity of the cryogels is 0.6 ± 0.1 EtBr molecule per nucleotide. Since the maximum amount of EtBr that can bind to DNA is one molecule per base pair, the results show that this value can be achieved using cryogels without disturbing the integrity of the gel structure.

Second series of binding tests were carried out by changing the external EtBr concentration between 0.005 and 1.3 mol EtBr per mole of nucleotide, and each experiment was carried out starting from freshly prepared swollen cryogel samples. The equilibrium data obtained after 5 days are illustrated in Fig. 7, where the EtBr binding efficiency (ε) of the cryogels and the mole ratio r of bound EtBr to nucleotide are plotted against the initial EtBr concentration $C_{f,o}$ in the solution. The efficiency was calculated as $\varepsilon = 1 - C_f/C_{f,o}$ where C_f is the concentration of EtBr in equilibrium with DNA cryogel. Even in very dilute solutions (down to concentrations as low as 3 μM), cryogels remove EtBr from aqueous solutions with an efficiency of 90%. After $r > 0.25$, corresponding to EtBr binding to DNA at every other base pair, efficiency starts to decrease below 90%.

In Fig. 8A, the mole ratio r of bound EtBr to nucleotide is plotted against the equilibrium EtBr concentration C_f in the solution. Increasing concentration of free EtBr leads to a rapid increase of the bound EtBr concentration. Then, the slope of the curve decreases and it approaches asymptotically the concentration of DNA binding sites n, indicating complete occupation of these binding sites. The data are also shown in Fig. 8B in the form of a Scatchard plot as r/C_f vs. r dependence. It is seen that, in the range of r between 0.005 and 0.2, a negative curvature appears in the

[1] For interpretation of color in Fig. 5, the reader is referred to the web version of this article.

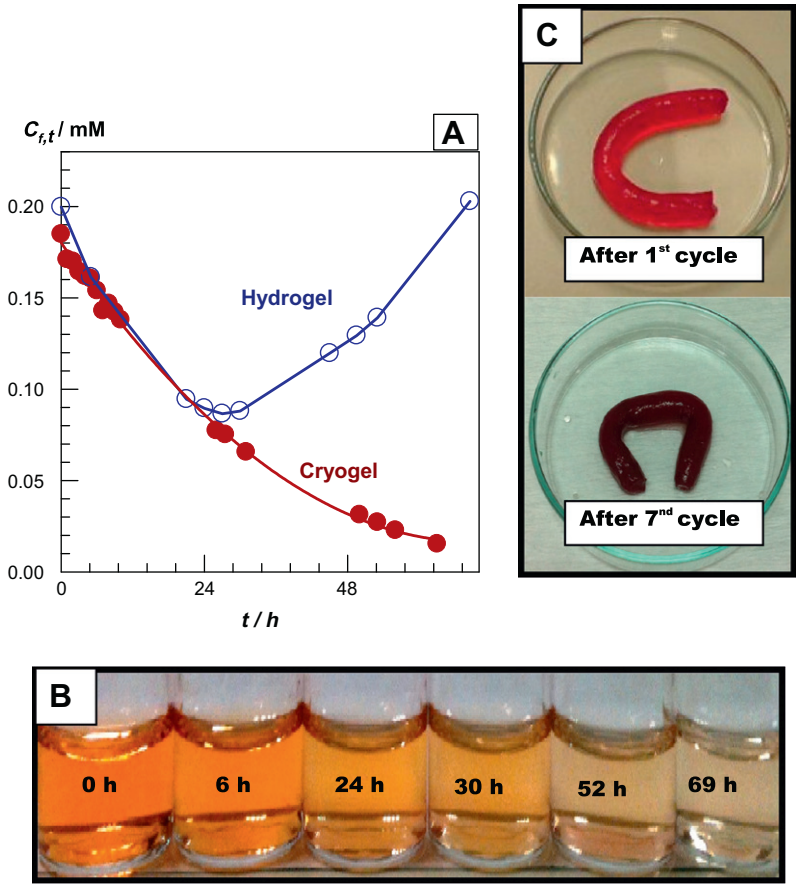

Fig. 5. (A) EtBr concentration ($C_{f,t}$) in the external solution plotted against the contact time t with the cryogel and hydrogel of DNA. (B) Images of the external EtBr solution at various times during the first absorption cycle using DNA cryogel. (C) Images of DNA cryogel after the first and seventh absorption cycles.

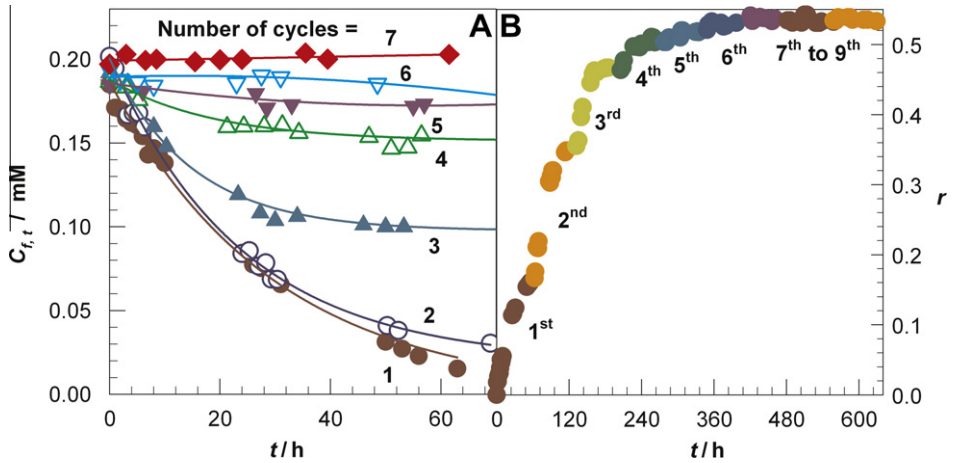

Fig. 6. (A) EtBr concentration ($C_{f,t}$) plotted against the contact time t for DNA cryogels. The results of seven successive sorption cycles are shown. (B) EtBr bound per nucleotide r plotted against the cumulative contact time t of nine successive cycles.

Scatchard plot. This is unexpected given that previous binding studies conducted in aqueous solutions at $r < 0.2$ resulted in straight lines with a positive and much higher slope, as represented in the figure by the dashed line [28–31]. Since any error in measuring C_f is amplified in r/C_f ratios, many points were taken at low C_f values and, several binding tests were carried out. However, in this range of r, r/C_f increased with r indicating that this behavior is real and should be related to the presence of DNA molecules within the gel network instead of in the solution.

Swelling behavior of the cryogels depending on the amount of bound EtBr per nucleotide is illustrated in Fig. 8C. Here, the normalized cryogel mass m_{rel} and volume V_{rel} with respect to those in pure water are shown as a function of r. At low ratios of bound EtBr to DNA ($r < 0.3$) the gel swells with increasing amount of bound EtBr. After a 3.5-fold increase in the volume and mass of the gel at $r = 0.3$, it starts to deswell again and finally attains a compact mass at $r = 0.6$. Equality of mass and volume changes of the cryogels demonstrates that this unusual swelling behavior is

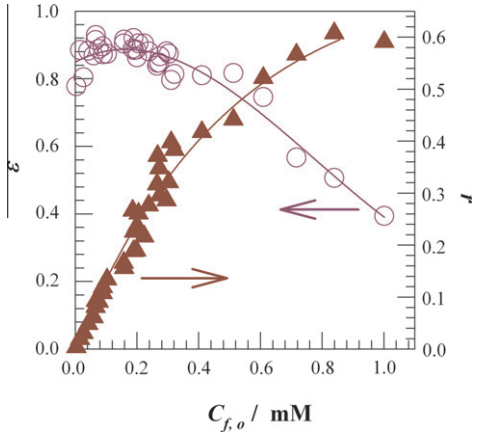

Fig. 7. EtBr binding efficiency ε of the cryogels and the mole ratio r of bound EtBr to nucleotide shown as a function of the initial EtBr concentration $C_{f,o}$.

related to the gel structure, but not the porosity changes depending on the EtBr binding.

To understand the observed phenomena, we should consider the nature of interactions of EtBr with nucleic acids in aqueous solutions. Previous studies indicate existence of mainly two types of EtBr binding to DNA [26–31]. At low values of r, EtBr binds strongly to DNA sites by intercalation, which appear to be saturated when one EtBr molecule is bound for every 2.1 ± 0.2 base pairs, i.e., $r = 0.24 \pm 0.02$. This is the accepted maximum value for intercalation based on the neighbor exclusion model. Sorption process of EtBr by the cryogels with 90% efficiency observed ar $r < 0.25$ is thus attributed to the intercalation of EtBr within the double helical DNA strands. Moreover, it was reported that the intercalation of EtBr into DNA changes the rotation angle between adjacent base pairs, and unwinds the helix, resulting in the lengthening of DNA [34,35]. This process also increases the viscosity of DNA solutions due to the increasing hydrodynamic size of DNA strands [54]. The extent of the increase of the viscosity depends on the number of EtBr molecules bound per nucleotide and, this behavior is also a characteristic of all DNA intercalators. Thus, the initial swelling of DNA gels at $r < 0.3$ may originate from increasing length of DNA network chains, decreasing the elastically effective crosslink density of the cryogels. We should mention that the disintegration of DNA hydrogels at $r = 0.10$–0.15 may also be related to this phenomenon (Fig. 5A). Lengthening and stiffening of the helix due to intercalated DNA may facilitate disruption of BDDE crosslinks [15,55], leading to the dissolution of DNA hydrogels in EtBr solutions. In contrast, cryogels are stable in EtBr solutions due to dense pore walls formed during cryoconcentration. The swelling response of DNA cryogels to changes in EtBr concentration between 3 and 300 μM also suggests that they can be used to detect DNA binding substrates in aqueous solutions. On the other hand, it was reported that at high r ratios ($r > 0.25$), after the primary sites of DNA have been filled, a secondary binding process occurs arising from electrostatic interactions between phosphate residues and EtBr molecules attached outside of the helix [32]. As a consequence, in this range of r, the cryogel deswells with increasing concentration of EtBr, which is similar to the behavior of polyelectrolyte hydrogels immersed in aqueous solutions of increasing salt concentration.

Equilibrium binding data given in Fig. 8A and B were analyzed by the Scatchard relation:

$$r/C_f = K(n - r) \tag{6}$$

where K is the binding constant and n is the maximum number of binding sites per nucleotide [37]. To reduce the effect of the data points recorded at low r values, experimental r and C_f data were fitted to Eq. (6a) which is simply a rearrangement of Eq. (6):

$$r = \frac{n}{1 + (K C_f)^{-1}} \tag{6a}$$

Solid lines in Fig. 8A and B are the best fit of Eq. (6a) to the data, yielding $K = 2.4\ (\pm 0.1) \times 10^4\ M^{-1}$ and $n = 0.65 \pm 0.02$. These binding parameters almost coincide with those reported in the literature for the secondary binding process of EtBr by DNA in aqueous solutions ($K = 2 \times 10^4\ M^{-1} - 8 \times 10^4\ M^{-1}$ and $n = 0.67$) [32].

At low r values ($r < 0.2$), since the major mode is intercalation, the rate of EtBr sorption by DNA is much faster. Reported values for the constant K are in the order of $10^6\ M^{-1}$ while the number of binding sites n decreases to about 0.25 [28–31]. The dashed line in Fig. 8B represents the intercalative type of EtBr binding by DNA using these parameters, which strongly deviates from the experimental data. We attribute this discrepancy to the fact that DNA strands in the present study are trapped inside a gel network, as compared to the previous works conducted in solutions. The concentration of mobile ions in polyelectrolyte gels is known to differ from that in the outer solution due to the fixed charges on the polymer network [56,57]. In case of DNA gels, fixed phosphate residues confined to the gel phase require equivalent number of counterions (Na^+) to stay within the gel to achieve electroneutrality. These counterions will always be there in excess of additional ions such as ethidium Et^+ and bromide Br^- diffusing into and out of the gel. Calculations for strong polyelectrolyte anionic gels similar to DNA gels show that at low concentration of 1:1 electrolytes, mobile ion concentration inside the gel is lower than its concentration

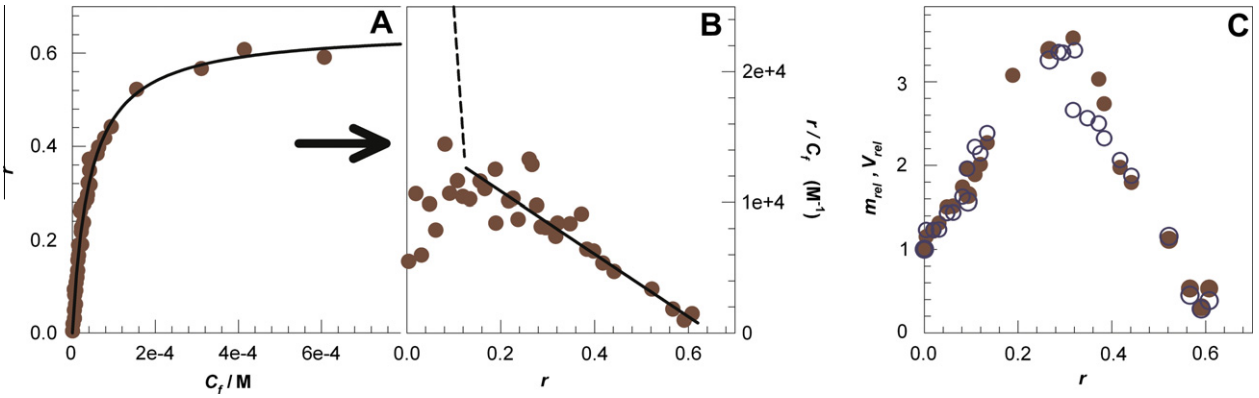

Fig. 8. (A) The mole ratio r of bound EtBr to nucleotide plotted against the concentration C_f of free EtBr in the solution. (B) Scatchard plot of the data in Fig. 8A as r/C_f vs. r dependence. (C) Relative gel mass m_{rel} (filled symbols) and volume V_{rel} (open symbols) of DNA cryogels shown as a function of r.

in the outer solution [57]. Thus, the actual concentration of free EtBr inside the gel in equilibrium with DNA is lower than the measured C_f values. At low C_f, the error introduced from this concentration difference is amplified in r/C_f ratios leading to the observed discrepancy.

4. Conclusions

We investigated the interaction of the DNA intercalator EtBr with the double helical network strands of DNA cryogels. The cryogels were prepared starting from aqueous DNA solutions at −18 °C using BDDE crosslinker and TEMED catalyst. Experiments conducted for structure optimization of the cryogels show that those formed at 5% DNA and 0.75% BDDE exhibit high-toughness combined with a high mechanical strength, which were used for EtBr binding studies. In contrast to the solubilization of DNA hydrogels in aqueous EtBr solutions, DNA cryogels remain stable in these solutions even after complete saturation of their EtBr binding sites. The total binding capacity of the cryogels was found to be 0.6 ± 0.1 EtBr molecule per nucleotide, which is close to the theoretical maximum number of EtBr molecules that can bind to DNA molecules. Even in very dilute solutions (down to concentrations as low as 3 μM), cryogels remove EtBr from aqueous solutions with an efficiency of 90%. After $r > 0.25$, corresponding to EtBr binding to DNA at every other base pair, efficiency starts to decrease below 90%. The equilibrium binding constant and the maximum number of EtBr binding sites of the cryogels estimated by the Scatchard relation almost coincide with the reported values for the secondary binding process of EtBr by DNA in aqueous solutions. At low mole ratios r of bound EtBr to DNA, the cryogels swell with increasing amount of bound EtBr which is attributed to the lengthening of the DNA network chains due to the intercalated EtBr. The response of DNA cryogels to changes in EtBr concentration between 3 and 300 μM also suggests that they can be used to detect DNA binding substrates in aqueous solutions.

Acknowledgements

Work was supported by the Scientific and Technical Research Council of Turkey (TUBITAK), TBAG -211T044. O.O. thanks Turkish Academy of Sciences (TUBA) for the partial support.

Appendix A. Supplementary material

Supplementary data associated with this article can be found, in the online version, at http://dx.doi.org/10.1016/j.reactfunctpolym.2012.11.014.

References

[1] J. Xu, T.H. LaBean, S.L. Craig, A. Ciferri (Eds.), Supramolecular Polymers, CRC Press, 2004, p. 445 (Chapter 12).
[2] V.A. Bloomfield, D.M. Crothers, I. Tinoco Jr., Nucleic Acids: Structures, Properties, and Functions, University Science Books, Sausalito, 2000.
[3] F.E. Alemdaroglu, A. Hermann, Org. Biomol. Chem. 5 (2007) 1311.
[4] O. Okay, J. Polym. Sci. B. Polym. Phys. 49 (2011) 551.
[5] Y. Murakami, M. Maeda, Biomacromolecules 6 (2005) 2927.
[6] N. Ishizuka, Y. Hashimoto, Y. Matsuo, K. Ijiro, Colloids Surf., A 284–285 (2006) 440.
[7] S.H. Um, J.B. Lee, N. Park, S.Y. Kwon, C.C. Umbach, Nat. Mater. 5 (2006) 797.
[8] T. Amiya, T. Tanaka, Macromolecules 20 (1987) 1162.
[9] N. Yonekura, H. Mutoh, Y. Miyagi, E. Takushi, Chem. Lett. 954 (2000).
[10] F. Topuz, O. Okay, Biomacromolecules 10 (2009) 2652.
[11] F. Horkay, P.J. Basser, Biomacromolecules 5 (2004) 232.
[12] D. Costa, M.G. Miguel, B. Lindman, J. Phys. Chem. B 111 (2007) 8444.
[13] D. Costa, M.G. Miguel, B. Lindman, J. Phys. Chem. B 111 (2007) 10886.
[14] H. Mayama, T. Nakai, E. Takushi, K. Tsujii, K. Yoshikawa, J. Chem. Phys. 127 (2007) 034901.
[15] D. Costa, M.G. Miguel, B. Lindman, Adv. Colloid Interface Sci. 158 (2010) 21.
[16] D. Costa, P. Hansson, S. Schneider, M.G. Miguel, B. Lindman, Biomacromolecules 7 (2006) 1090.
[17] F. Topuz, O. Okay, Macromolecules 41 (2008) 8847.
[18] N. Orakdogen, B. Erman, O. Okay, Macromolecules 43 (2010) 1530.
[19] N. Orakdogen, P. Karacan, O. Okay, React. Funct. Polym. 71 (2011) 782.
[20] M.J. Waring, Annu. Rev. Biochem. 50 (1981) 159.
[21] J.B. Chaires, Anti-Cancer Drugs 11 (1996) 569.
[22] J.B. Chaires, Curr. Opin. Struct. Biol. 8 (1998) 314.
[23] L.S. Lerman, J. Mol. Biol. 3 (1961) 18.
[24] R. Palchaudhuri, P.J. Hergenrother, Curr. Opin. Biotechnol. 18 (2007) 497.
[25] J.-B. LePecq, P. Yot, C. Paoletti, C.R. Acad. Sci. 259 (1964) 1786.
[26] M.J. Waring, J. Mol. Biol. 13 (1965) 269.
[27] J.-B. LePecq, C. Paoletti, J. Mol. Biol. 27 (1967) 87.
[28] F.M. Pohl, T.M. Jouin, W. Baehr, J.J. Holbrook, Proc. Natl. Acad. Sci. USA 69 (1972) 3805.
[29] C.G. Reinhardt, T.R. Krugh, Biochemistry 17 (1978) 4845.
[30] D.M. Hinton, V.C. Bode, J. Biol. Chem. 250 (1975) 1061.
[31] S. Aktipis, A. Kindelis, Biochemistry 12 (1973) 1213.
[32] S.H. Minasyan, L.A. Tavadyan, A.P. Antonyan, H.G. Davtyan, M.A. Parsadanyan, P.O. Vardevanyan, Bioelectrochemistry 68 (2006) 48.
[33] A. Celedon, D. Wirtz, S. Sun, J. Phys. Chem. B. 114 (2010) 16929.
[34] H.M. Sobell, C.C. Tsai, S.C. Jain, S.G. Gilbert, J. Mol. Biol. 114 (1977) 333.
[35] H.M. Berman, P.R. Young, Annu. Rev. Biophys. Bioeng. 10 (1981) 87.
[36] N. Gundogan, D. Melekaslan, O. Okay, Macromolecules 35 (2002) 5616.
[37] G. Scatchard, Ann. N.Y. Acad. Sci. 51 (1949) 660.
[38] M. Rosa, R. Dias, M.G. Miguel, B. Lindman, Biomacromolecules 6 (2005) 2164.
[39] M. Eriksson, S.K. Kim, S. Sen, A. Graslund, B. Jernstrom, B. Norden, J. Am. Chem. Soc. 115 (1993) 1639.
[40] M. Koskinen, K. Plna, Chem.-Biol. Interact. 129 (2000) 209.
[41] R.V. Ivanov, T.A. Babushkina, V.I. Lozinsky, Polym. Sci. Ser. A 47 (2005) 791.
[42] R.V. Ivanov, V.I. Lozinsky, Polym. Sci. Ser. A 48 (2006) 1232.
[43] F.M. Plieva, M. Karlsson, M.-R. Aguilar, D. Gomez, S. Mikhalovsky, I.Y. Galaev, Soft Matter 1 (2005) 303.
[44] F. Plieva, X. Huiting, I.Y. Galaev, B. Bergenstahl, B. Mattiasson, J. Mater. Chem. 16 (2006) 4065.
[45] V.I. Lozinsky, Russ. Chem. Rev. 71 (2002) 489.
[46] M.M. Ozmen, O. Okay, Polymer 46 (2005) 8119.
[47] M.V. Dinu, M.M. Ozmen, E.S. Dragan, O. Okay, Polymer 48 (2007) 195.
[48] F. Plieva, I.N. Savina, S. Deraz, J. Andersson, I.Y. Galaev, B. Mattiasson, J. Chromatogr. Sci. 807 (2004) 129.
[49] O. Okay, Prog. Polym. Sci. 25 (2000) 711.
[50] V.I. Lozinsky, I.Y. Galaev, F.M. Plieva, I.N. Savina, H. Jungvid, B. Mattiasson, Trends in Biotechnol. 21 (2003) 445.
[51] S.L. Lee, P.G. Debenedetti, J.R. Errington, B.A. Pethica, D.J. Moore, J. Phys. Chem. B 108 (2004) 3098.
[52] H. Matsuno, J.-I. Nakahara, K. Tanaka, Biomacromolecules 12 (2011) 173.
[53] D.R. Whelan, K.R. Bambery, P. Heraud, M.J. Tobin, M. Diem, D. McNaughton, B.R. Wood, Nucleic Acids Res. 39 (2011) 5439.
[54] K. Faulhaber, A. Granzhan, H. Ihmels, D. Otto, L. Thomas, S. Wells, Photobiol. Sci. 10 (2011) 1535.
[55] C. Staples, R. Boatman, M. Cano, Chemosphere 36 (1998) 1585.
[56] U.P. Schroder, W. Oppermann, J.P. Cohen-Addad (Eds.), Physical Properties of Polymeric Gels, John Wiley, 1996, p. 19 (Chapter 2).
[57] S. Durmaz, O. Okay, Polymer 41 (2000) 3693.